INFECTION AND IMMUNITY, Aug. 2005, p. 4653–4667 Vol. 73, No. 8
0019-9567/05/$08.00+0 doi:10.1128/IAI.73.8.4653–4667.2005

Illustration of Pneumococcal Polysaccharide Capsule during Adherence and Invasion of Epithelial Cells

Sven Hammerschmidt,[1,2]* Sonja Wolff,[2] Andreas Hocke,[3] Simone Rosseau,[3] Ellruth Müller,[2] and Manfred Rohde[2]

Research Center for Infectious Diseases, University of Würzburg, D-97070 Würzburg, Germany[1]; Department of Microbial Pathogenicity, GBF-German Research Centre for Biotechnology, D-38124 Braunschweig, Germany[2]; and Department of Internal Medicine/Infectious Diseases, Charité-University Medicine Berlin, 13353 Berlin, Germany[3]

Received 16 September 2004/Returned for modification 24 November 2004/Accepted 16 March 2005

The capsular polysaccharide of *Streptococcus pneumoniae* represents an important virulence factor and protects against phagocytosis. In this study the amount of capsular polysaccharide present on the bacterial surface during the infection process was illustrated by electron microscopic studies. After infection of A549 cells (type II pneumocytes) and HEp-2 epithelial cells a modified fixation method was used that allowed visualization of the state of capsule expression. This modified fixation procedure did not require the use of capsule-specific antibodies. Visualization of pneumococci in intimate contact and invading cells demonstrated that pneumococci were devoid of capsular polysaccharide. Pneumococci not in contact with the cells did not show alterations in capsular polysaccharide. After infection of the cells, invasive pneumococci of different strains and serotypes were recovered. Single colonies of these recovered pneumococci exhibited an up-to-10^5-fold-enhanced capacity to adhere and an up-to-10^4-fold-enhanced capacity to invade epithelial cells. Electron microscopic studies using a lysine-ruthenium red (LRR) fixation procedure or cryo-field emission scanning electron microscopy revealed a reduction in capsular material, as determined in detail for a serotype 3 pneumococcal strain. The amount of polysaccharide in the serotype 3 capsule was also determined after intranasal infection of mice. This study illustrates for the first time the phenotypic variation of the polysaccharide capsule in the initial phase of pneumococcal infections. The modified LRR fixation allowed monitoring of the state of capsule expression of pathogens during the infectious process.

Streptococcus pneumoniae is a commensal of the human respiratory tract, but it also causes local infections and serious life-threatening diseases, such as pneumonia, sepsis, and meningitis (4, 9, 34, 45). The initial phase of pathogenesis of mucosal microorganisms is associated with colonization, followed by intimate contact with host cells, which promotes uptake. The successful conversion of a commensal to an invasive microorganism is accompanied by the transmigration of tissue barriers and the subsequent adaptation of the pathogen to different host niches. This process is a multifunctional and highly regulated process (18).

Pneumococci of different serotypes are able to simultaneously colonize the nasopharynges of healthy individuals (20). Translocation of the mucosal barrier and dissemination within the host lead to serious invasive diseases. However, disease is most commonly due to strains representing 20 of the >90 different serotypes (33, 34). Pneumococci adhere to and invade different epithelial cells, as well as endothelial cells, using cell-specific mechanisms for internalization (1, 11, 14, 38, 42, 56). Previous studies and in vivo experiments with animal infection models also suggested that the capsular polysaccharide might influence the proportion of bacteria attaching to and entering the cells (44). The significance of capsule modulation during the transition from carriage to invasive disease has already been demonstrated for another pathogen belonging to the normal microflora of the nasopharynx. In *Neisseria meningitidis* the "phase-off" of capsule production enhances tissue invasion, and phase-on is essential for survival in systemic infections (21). The occurrence of pneumococcal colonial variants along with their phenotypic appearance as opaque and transparent colonies as a result of opacity phase variation has been associated with different levels of capsule expression (26, 50). The spontaneous variation of colonial morphology to the transparent phenotype is linked with reduced expression of capsular polysaccharide and an enhanced ability of this phenotype for nasopharyngeal colonization (50). The significance of the polysaccharide capsule for pneumococcal pathogenesis, which renders the pneumococcus resistant to complement-mediated opsonophagocytosis and plays a key role in systemic dissemination, has been studied in detail (3, 5, 8, 22, 25, 46, 49, 55). Encapsulated pneumococci also have an advantage in colonization of the nasopharynx, although substantially reduced levels of capsule, compared to wild-type levels, are sufficient for murine carriage (30).

The molecular mechanisms involved in the regulation of pneumococcal capsule expression have also been addressed. Recombinant exchanges and spontaneous sequence duplications in type 3-specific genes have been identified as the causes of high-frequency serotype and phase variations, respectively (10, 47, 48).

In this paper we describe the phenotypic and morphological variation with respect to the polysaccharide capsule in the initial phase of the infection. In conjunction with scanning and transmission electron microscopy, a modified fixation method was used in order to illustrate the amount of capsule present

* Corresponding author. Mailing address: Research Center for Infectious Diseases, University of Würzburg, Röntgenring 11, 97070 Würzburg, Germany. Phone: 0049-(0)931-31 2153. Fax: 0049-(0)931-31 2578. E-mail: s.hammerschmidt@mail.uni-wuerzburg.de.

during adherence and uptake of pneumococci. Our results suggested that pneumococci which are in intimate contact with cells and in the process of entering the cells are devoid of a polysaccharide capsule. Invasive pneumococci which had entered the cells were recovered. Electron microscopic studies of recovered pneumococci indicated that there was a loss of capsular polysaccharide material. The effect of capsule loss was demonstrated by comparing the attachment and invasion of single colonies of recovered pneumococci belonging to different serotypes to the attachment and invasion of the corresponding wild-type strain.

MATERIALS AND METHODS

Bacterial strains and cell culture. Clinical isolates of *S. pneumoniae* provided by the Statens Serum Institute, Copenhagen, Denmark, and the Medical University, Düsseldorf, Germany, defined pneumococcal strains from the American Type Culture Collection and the National Collection of Type Cultures, *S. pneumoniae* A66 (serotype 3) (6), *S. pneumoniae* D39, a capsular serotype 2 strain, and its nonencapsulated derivative R6x (43), as well as the nonencapsulated strain R800 (derived from R36A), were used in this study. Strains were cultured on blood agar (Merck) or in Todd-Hewitt broth (Oxoid, Basingstoke, England) supplemented with 0.5% yeast extract to a cell density of 5×10^8 CFU/ml and used in cell culture infection experiments. The human lung alveolar carcinoma epithelial cell line A549 (type II pneumocytes; ATCC CCl-185) and the HEp-2 larynx carcinoma cell line (ATCC CCL-23) were grown in Dulbecco's modified Eagle's medium (DMEM) supplemented with 10% fetal calf serum (Sigma), 5 mM glutamine, penicillin G (100 U ml^{-1}), and streptomycin (100 $\mu g,ml^{-1}$) (all from GIBCO BRL) at 37°C under 5% CO_2.

Epithelial adherence and invasion assay. Pneumococcal adherence and invasion assays with epithelial cells were performed in 24-well plates (Greiner, Germany). Confluent epithelial cells (approximately 1×10^5 cells) were inoculated with 5×10^6 pneumococci and incubated in Dulbecco's minimal essential medium-HEPES at 37°C in the presence of 5% CO_2 for 3 h. Subsequently, the cells were rinsed several times with phosphate-buffered saline (PBS) to remove unbound bacteria. For isolation of pneumococci that were taken up by the cells, extracellular bacteria were killed by treatment with gentamicin (200 $\mu g\ ml^{-1}$) and penicillin G (10 $\mu g\ ml^{-1}$). The intracellular pneumococci were recovered after washing by saponin-mediated lysis (1% [wt/vol] saponin) of the cells and plated on blood agar plates. The amount of intracellular surviving bacteria per well was determined (data not shown). When appropriate, survivors were isolated, collected, and reused in the invasion assay. In addition, the numbers of adherent and invasive pneumococci were determined by immunofluorescence microscopy.

Immunofluorescence microscopy. Cells with adherent and intracellular bacteria were fixed in 3.7% paraformaldehyde on glass coverslips (diameter, 12 mm). Extracellular bacteria which were bound to epithelial cells were incubated for 30 min with an antipneumococcal antiserum (diluted 1:100 in PBS) which was generated in a rabbit against heat-inactivated pneumococci (R6x and ATCC 11733) and reacted equally well with different pneumococcal strains (14). The reactivity of the antipneumococcal antiserum against encapsulated pneumococci and variants was determined using a fluorescence-based antibody titration protocol. Briefly, different amounts of bacteria were incubated with serial dilutions of the antiserum, and this was followed by incubation with a fluorescein isothiocyanate-labeled goat anti-rabbit immunoglobulin (Dianova). Fluorescence was measured at 485 nm (excitation) and 538 nm (emission) using a Fluoroskan Ascent (ThermoLabsystems). The immunoreactivity of highly encapsulated bacteria (e.g., A66 type 3) was fourfold lower than that of a nonencapsulated pneumococcal variant or nonencapsulated pneumococci. The applied dilution (1:100) of the antipneumococcal antiserum efficiently stained encapsulated phenotypes (serotype 3), as confirmed by immunofluorescence microscopy (data not shown). The infected cells were washed three times with PBS, and extracellular bacteria were incubated with a fluorescein isothiocyanate-labeled goat anti-rabbit immunoglobulin (Dianova). After permeabilization with 0.1% Triton X-100 for 5 min, the extracellular and intracellular pneumococci were stained using antipneumococcal antiserum and tetramethyl rhodamine isocyanate-labeled goat anti-rabbit immunoglobulin (Dianova). Extracellular pneumococci were yellow (green/red), and intracellular pneumococci were red. Bacterial adherence and invasion were scored for at least 50 cells per glass coverslip by fluorescence microscopy. Each experiment in this study was repeated at least five times, and the mean ± standard deviation was calculated.

Electron microscopy. (i) Field emission scanning electron microscopy (FESEM). For the conventional fixation procedure, infected monolayers grown on coverslips were fixed with a fixation solution containing 5% formaldehyde and 2% glutaraldehyde in cacodylate buffer (0.1 M cacodylate, 0.01 M $CaCl_2$, 0.01 M $MgCl_2$, 0.09 M sucrose; pH 6.9) for 1 h on ice and subsequently washed several times with cacodylate buffer.

For the formaldehyde-glutaraldehyde ruthenium red-osmium fixation method, pneumococci were fixed in a fixation solution containing 3% glutaraldehyde and 0.15% ruthenium red in cacodylate buffer for 1 h on ice. After washing in cacodylate buffer containing 0.15% ruthenium red, samples were fixed in 1% osmium in cacodylate buffer containing 0.15% ruthenium red for 1 h at room temperature and washed with cacodylate buffer with 0.15% ruthenium red.

For the lysine-acetate-based formaldehyde-glutaraldehyde ruthenium red-osmium fixation procedure (LRR fixation), infected monolayers were first fixed with 2% formaldehyde and 2.5% glutaraldehyde in cacodylate buffer containing 0.075% ruthenium red and 0.075 M lysine-acetate for 20 min on ice. After washing with cacodylate buffer containing 0.075% ruthenium red, samples were fixed a second time with 2% formaldehyde and 2.5% glutaraldehyde in cacodylate buffer with 0.075% ruthenium red for 3 h, washed with cacodylate buffer containing 0.075% ruthenium red, and then fixed with 1% osmium in ruthenium red containing cacodylate buffer for 1 h at room temperature. Subsequently, samples were washed several times with ruthenium red-cacodylate buffer.

All samples were then dehydrated with a graded series of acetone (10, 30, 50, 70, 90, and 100%) on ice for 15 min for each step. Samples in the 100% acetone step were allowed to reach room temperature before another change of 100% acetone. Samples were then subjected to critical-point drying with liquid CO_2 (CPD030; Balzers, Liechtenstein). The dried samples were covered with an approximately 10-nm-thick gold film by sputter coating (SCD040; Balzers Union, Liechtenstein) before examination with a field emission scanning electron microscope (Zeiss DSM 982 Gemini) using an Everhart Thornley SE detector and an in-lens detector at a 50:50 ratio at an acceleration voltage of 5 kV.

(ii) Transmission electron microscopy. For morphological analysis of the capsule structure, samples were fixed by the LRR fixation procedure (see above). Samples were then dehydrated with a graded series of ethanol (10, 30, 50, 70, 90, and 100%) on ice for 30 min for each step. Samples were infiltrated with the acrylic resin LRWhite by applying 1 part 100% ethanol and 1 part LRWhite for 2 h on ice, followed by 1 part ethanol and 2 parts LRWhite and overnight incubation on ice. The next day pure resin was added, and samples were incubated for 8 h on ice, changed, and left overnight. Finally, samples were placed in gelatin capsules, which were filled with pure LRWhite resin at room temperature. The LRWhite resin was polymerized for 48 h at 60°C. Ultrathin sections were cut with a diamond knife, and sections were picked up with Formvar-coated copper grids (300 mesh). Counterstaining of the sections was performed with 4% aqueous uranyl acetate for 5 min. After air drying, samples were examined with a Zeiss EM 910 transmission electron microscope at an acceleration voltage of 80 kV.

(iii) Cryo-FESEM. For cryo-FESEM samples were centrifuged, and 2 μl of each pellet was applied to a brass sample holder (Balzers, Liechtenstein) and immediately frozen in melting nitrogen. Frozen samples were then transferred into a cryo-unit (Oxford HF1500), freeze fractured at −110°C, and freeze-etched for 30 s at −110°C. After sputter coating with a thin layer of gold-palladium, samples were transferred onto a cryo-stage inside a Zeiss DSM982 Gemini field emission scanning microscope and examined at −135°C at an acceleration voltage of 2 kV.

Capsule measurement. Quelling (agglutination) reactions were performed using capsule type 3-specific antiserum (Statens Serum Institute, Copenhagen, Denmark). Cell-associated capsule production and cell-released polysaccharides were determined using the Stains-all assay (Sigma) for detecting acidic polysaccharides (30, 39). Pneumococci were cultured in semisynthetic medium (C+Y) to a cell density of 4×10^8 cells/ml (27), and the bacteria and culture supernatant were separated by centrifugation. Bacteria were washed twice with PBS, and 2.5×10^9 pneumococci were resuspended in 0.5 ml water. The content of bacterium-associated polysaccharides or the amount of polysaccharides in 0.5 ml of culture supernatant was determined by measuring the absorbance at 640 nm after addition of 2 ml of a solution containing 20 mg of 1-ethyl-2[3-(1-ethylnaphtho-[1,2-*d*]thiazolin-2-ylidene)-2methylpropenyl]naphtho-[1,2-*d*]thiazolium bromide (Stains-all) and 60 μl of glacial acetic acid in 100 ml of 50% formamide. Values were normalized by subtraction of values measured for culture medium or water.

Intranasal challenge of mice and isolation of lungs. Pathogen-free C57BL/6 mice were obtained from Charles River (Sulzfeld, Germany). Female inbred mice were challenged when they were ~10 weeks old and weighed ~19 g. Mice were anesthetized by intraperitoneal injection of 40 μl of a 5:2 mixture of ketamine (50 mg/ml) and xylazine (2%) and were challenged with 20 μl of sterile

TABLE 1. Adherence to A549 cells by selected *S. pneumoniae* clinical isolates, defined strains, and variants[a]

Strain	Strain derivation and properties	No. of adherent CFU per 10^5 cells [mean (SE)]
P52	Type 1, ATCC 12213 (I-192R)	34.2 (12.8)
P53	Type 1, SSI[b]	54.3 (19.4)
P53 variant	Recovered from epithelial cell line	93.2×10^5 (37.3×10^5)
D39	Type 2	17.5 (4.5)
P51	Type 2, ATCC 11733	5.1×10^5 (2.4×10^5)
A66	Type 3[c]	28.8 (10.9)
A66 variant	Recovered from epithelial cell line	255.5×10^5 (111.3×10^5)
P54	Type 3, SSI	38.0 (23.2)
P85	Type 3, blood isolate, MUD[d]	154.8 (22.6)
P85 variant	Recovered from epithelial cell line	19.8×10^5 (11.3×10^5)
P105	Type 4, blood isolate, MUD, pneumonia	132.3 (29.1)
P76	Type 6A, blood isolate, MUD, pneumonia	274.0 (98.3)
P93	Type 6B, blood isolate, MUD	683.5 (193.6)
P88	Type 7F, blood isolate, MUD, pneumonia	344.5 (92.8)
P65	Type 9A, blood isolate, MUD, meningitis	29.5 (19.6)
P72	Type 14, blood isolate, MUD, pneumonia	2.00×10^5 (1.6×10^5)
P80	Type 14, blood isolate, MUD, pneumonia	138.0 (42.4)
P84	Type 14, blood isolate, MUD, pneumonia	9.0 (8.5)
P104	Type 14, CSF isolate, MUD, meningitis	12.3 (8.6)
P92	Type 18B, blood isolate, MUD, pneumonia	4.4×10^5 (3.0×10^5)
P107	Type 18F, blood isolate, MUD, pneumonia	4.9×10^5 (2.4×10^5)
P91	Type 19F, blood isolate, MUD	31.0 (12.2)
P91 variant	Recovered from epithelial cell line	508.0 (171.4)
P103	Type 19F, blood isolate, MUD, pneumonia	5.3 (3.6)
P102	Type 23A, cerebrospinal fluid isolate, MUD, meningitis	14.5 (7.2)
P133	Type 6A, respiratory tract isolate, MUD	94.3×10^5 (27.8×10^5)
P134	Type 21, respiratory tract isolate, MUD	5.2×10^5 (0.5×10^5)
R6x	Nonencapsulated derivate of D39	4.4×10^5 (1.4×10^5)
R800	Nonencapsulated	125.0×10^5 (25.0×10^5)

[a] *S. pneumoniae* strains were used to infect A549 epithelial cells (type II pneumocytes) at a ratio of 50:1. The number of attached bacteria was determined by immunofluorescence microscopy for at least 50 epithelial cells. The data are means ± standard errors of at least five independent experiments. The adherence of HEp-2 cells was in the same range as the adherence to A549 cells (data not shown). The serotype, source of isolation, and, if possible, the disease caused by the clinical isolate are indicated.

[b] SSI, Statens Serum Institute, Copenhagen, Denmark.

[c] See reference 6.

[d] MUD, Medical University of Düsseldorf, Düsseldorf, Germany.

PBS containing 5×10^6 CFU of serotype 3 *S. pneumoniae* (A66) administered in the nostrils. Control mice received 20 μl of sterile PBS without bacteria. Infected mice were sacrificed after 3 h, PBS-instilled control mice were sacrificed after 6 h, and lungs were processed for electron microscopy. The trachea was dissected, and a tracheal cannula was immediately inserted. Subsequently, mechanical ventilation was started with ambient air using a mouse respirator (Mini Vent type 845; Hugo Sachs Elektronik, March-Hugstetten, Germany). A median laparotomy and incision of the diaphragm were performed, and the mice were anticoagulated intracardially with 40 U of heparin. After midsternal thoracotomy the apex of the heart was cut off to allow blood outflow. After this, the lungs were instilled with 2% formaldehyde and 2.5% glutaraldehyde in cacodylate buffer containing 0.075% ruthenium red and 0.075 M lysine-acetate for 20 min at 4°C. The lungs were further fixed by using the LRR fixation procedure and then embedded by using the protocol of Spurr (41).

RESULTS

Adherence of clinical *S. pneumoniae* strains. *S. pneumoniae* strains isolated from blood, cerebrospinal fluid, and the respiratory tract, as well as defined pneumococcal strains, were used for adherence studies. Bacteria were used to infect A549 cells at a ratio of 50:1. The numbers of pneumococci attached to the epithelial cells were determined by immunofluorescence. The ability to adhere to the epithelial cells varied among clinical strains belonging to different serotypes. The levels of adherence of strains of the same serotype obtained from the same source of isolation (e.g., type 14) were also not in the same range (Table 1). The type 14 strain P72, which adhered efficiently to A549 cells, produced smaller amounts of bacterium-associated polysaccharides than other type 14 strains (e.g., P84) (data not shown). Strikingly, respiratory tract isolates and some pneumonia isolates were as efficient as the nonencapsulated strains R6x and R800, respectively, and defined strain ATCC 11733 (serotype 2), which is low encapsulated (Fig. 1 and Table 1).

Invasiveness of pneumococci recovered from epithelial cells. HEp-2 and/or A549 epithelial cells were infected with *S. pneumoniae*, and the invasive bacteria were isolated and enriched by using the gentamicin assay. The efficiency of single colonies of these recovered pneumococci for invading cells was compared to that of the original parental strains. Recovered cells of *S. pneumoniae* serotype 1, serotype 3 (strain A66 and blood isolate P85), and serotype 19F (blood isolate P91) were used to compare the effects of epithelial cell culture invasion (Table 1). The results demonstrated that the recovered pneumococci were significantly more efficient in binding to and invading epithelial cells than their parental counterparts (Fig. 1 and Table 1). The recovered bacteria which were derived from low-invasive-potential parental pneumococci belonging to different serotypes were designated in the subsequent experiments variants of the corresponding wild-type strains.

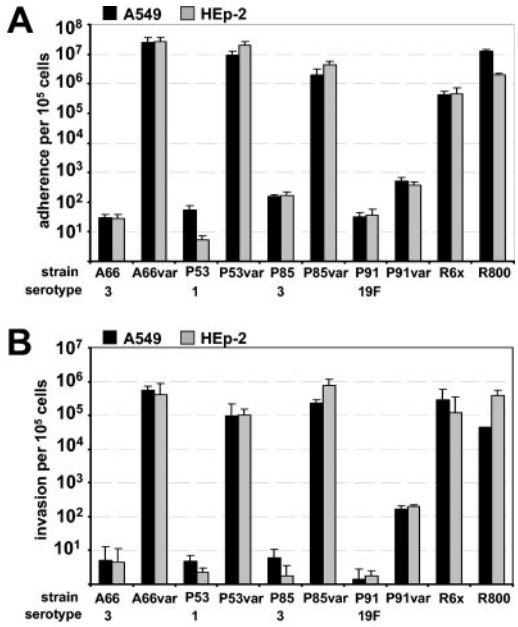

FIG. 1. Efficiency of adherence and invasion of pneumococcal variants recovered from epithelial cells. Equal amounts of wild-type pneumococci and their variants were used in the cell culture infection assay. Adherence (A) and invasion (B) were measured microscopically by double immunofluorescence. var, recovered pneumococci. The data are the means ± standard errors of five independent experiments.

On blood agar pneumococcal variants of serotype 3 strain A66 (A66 variants) showed an altered mucoid capsular phenotype compared to strain A66. The invasive capacity of single colonies of these A66 variants exceeded that of the parental strain by 10^4-fold, irrespective of whether the number of invasive bacteria was scored microscopically (Fig. 1) or by gentamicin selection (data not shown). Similarly, the number of adhesive pneumococci of these variants increased 10^5-fold (Fig. 1). This was observed for individually selected single colonies which were isolated after the gentamicin assay (data not shown). The phenotypic alteration of the mucoid phenotype and the results of the infection assays suggested that the high invasiveness of the variants may have been due to the loss of capsular material.

Development of fixation methods for electron microscopic studies to maintain capsular polysaccharide structure. The capsule of pneumococci is considered to be an anionic matrix which is highly hydrated. These characteristics make its stabilization and visualization for electron microscopic studies difficult. Conventional aldehyde fixation, osmification, and dehydration with ethanol or acetone always resulted in loss of capsular material when samples were analyzed in FESEM studies (Fig. 2A) or by using ultrathin sections (Fig. 2B). The introduction of ruthenium red, a cationic chemical which reacts strongly with anionic moieties (17, 28, 29, 40), resulted in better, but nevertheless unsatisfactory, preservation of the pneumococcal capsular structure. As deduced from Fig. 2, treatment of wild-type pneumococci with ruthenium red during the fixation process resulted in retention of some capsular material on the bacterial surface (Fig. 2C and D) compared to conventional fixation with aldehydes (Fig. 2A and B). Fassel et al. (15, 16) demonstrated that addition of lysine in combination with ruthenium red resulted in better preservation of the staphylococcal glycocalyx than ruthenium red fixation alone. Therefore, we modified the previously described fixation methods and devised a fixation protocol that resulted in a very well-preserved capsule for scanning and transmission electron microscopic studies. The addition of lysine-acetate to the fixation solution (LRR fixation) and carrying out the primary fixation for only 20 min resulted in much more pronounced capsule preservation, especially in ultrathin sections after embedding in LRWhite resin (Fig. 2E and F). Nevertheless, due to dehydration of the samples for FESEM, the highly hydrated capsular structure collapsed (Fig. 2E). However, comparison of the capsule structure to nonencapsulated pneumococci revealed significant differences which allowed us to discriminate both strains clearly in the FESEM analysis (Fig. 3A to C). The LRR fixation method followed by FESEM analysis was therefore considered a useful method for discriminating between nonencapsulated and encapsulated pneumococci.

Illustration of polysaccharide capsule by cryo-FESEM. To obtain information on the "natural" hydrated state of the pneumococci capsule, we performed cryo-FESEM studies of pneumococci after LRR fixation. In Fig. 4 the dense thick layer of capsular material of serotype 3 strain A66 surrounding the pneumococcus is clearly visible.

***S. pneumoniae* A66 variants recovered from epithelial cells: state of capsule expression.** The amount of the polysaccharide capsule of recovered *S. pneumoniae* A66 variants was investigated by employing the LRR fixation method and cryo-FESEM after LRR fixation. As demonstrated by conventional FESEM, pneumococcal A66 variants isolated from HEp-2 cells (Fig. 3B) or A549 cells (Fig. 3C) did not exhibit a capsular layer around the surface compared to the parental strain A66 (Fig. 3A), and so the results clearly demonstrated that bacteria recovered from the intracellular cell environment were nonencapsulated. These differences between parental strain A66, which is highly encapsulated (Fig. 3D), and A66 variants (Fig. 3E and F) were also observed in cyro-FESEM studies which allowed us to observe the capsule in its vitrified state. Ultrathin sections of LRR-fixed pneumococci were examined by using LRWhite-embedded samples. Again, the parental strain exhibited a dense and thick capsule (Fig. 3G). In contrast, variants showed no visible capsular structures (Fig. 3H and I). The decreased amounts of capsular polysaccharides of other variants compared to wild-type strains (e.g., serotype 1 or 19F) were also detectable when the LRR fixation protocol was used (Fig. 5, compare panels A and B or panels C and D). The variants exhibited only small amounts of polysaccharides, which were comparable with the amounts observed for nonencapsulated strains R6x (Fig. 5E) and R800 (Fig. 5F) after LRR fixation.

Capsular polysaccharide production. The amounts of capsular polysaccharide produced by wild-type pneumococci and pneumococcal variants recovered from epithelial cells were assessed by a quantitative assay that measured amounts of polysaccharides. Of the strains tested, the variants of serotype 3 strains (A66 variant and P85 variant) and serotype 1 (P53 variant) showed substantially decreased amounts of bacterium-associated polysaccharides compared to the wild-type strains. The amounts of polysaccharides in culture supernatants were

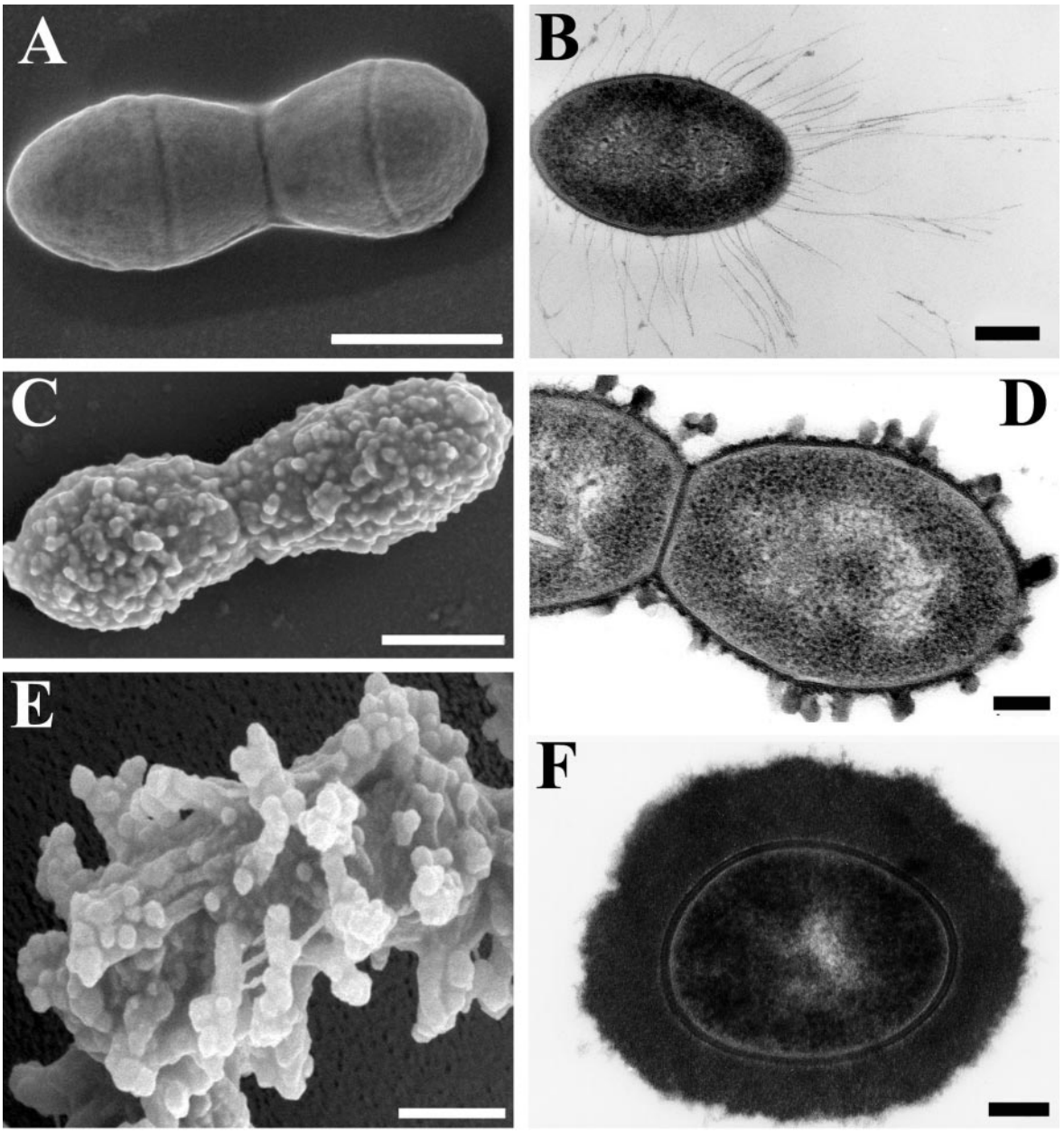

FIG. 2. Comparison of different fixation methods for visualization of the capsule. Conventional fixation with formaldehyde and glutaraldehyde resulted in a total loss of the capsule of serotype 3 pneumococcus strain A66, as demonstrated by FESEM (A) and in ultrathin sections (B). Addition of ruthenium red in the fixation protocol resulted in some remaining structural material of the capsule on the pneumococcal surface (C and D). A well-preserved capsular structure was observed when a lysine-acetate-based ruthenium red-osmium fixation protocol was used (E and F). (A, C, and E) Bars = 0.5 μm. (B, D, and F) Bars = 0.1 μm.

substantially reduced for the serotype 3 A66 and P85 variants (Fig. 6). The quelling reaction using capsule type 3-specific antiserum revealed agglutination for the A66 strain, but no agglutination was observed for the A66 variants. The variants showed no swelling reaction, confirming the substantially reduced amount of bacterium-associated capsular polysaccharide material.

Phenotypic visualization of capsule expression during invasion by high-resolution scanning electron microscopy. The LRR fixation protocol and subsequent preparation for FESEM were then employed to observe at high resolution the state of encapsulation during adhesion and invasion. As shown in Fig. 7, a time series demonstrated that during adhesion of *S. pneumoniae* to the HEp-2 host cells the thickness of the pneumococcal capsule was reduced. Pneumococcus strain A66 was used as a representative type 3 strain. The reduction in encapsulation was greatest when the bacteria were in intimate direct contact with the host cell membrane. After 30 min of infection there were no clearly detectable differences between the capsule structure of adherent pneumococci (Fig. 7A and B and

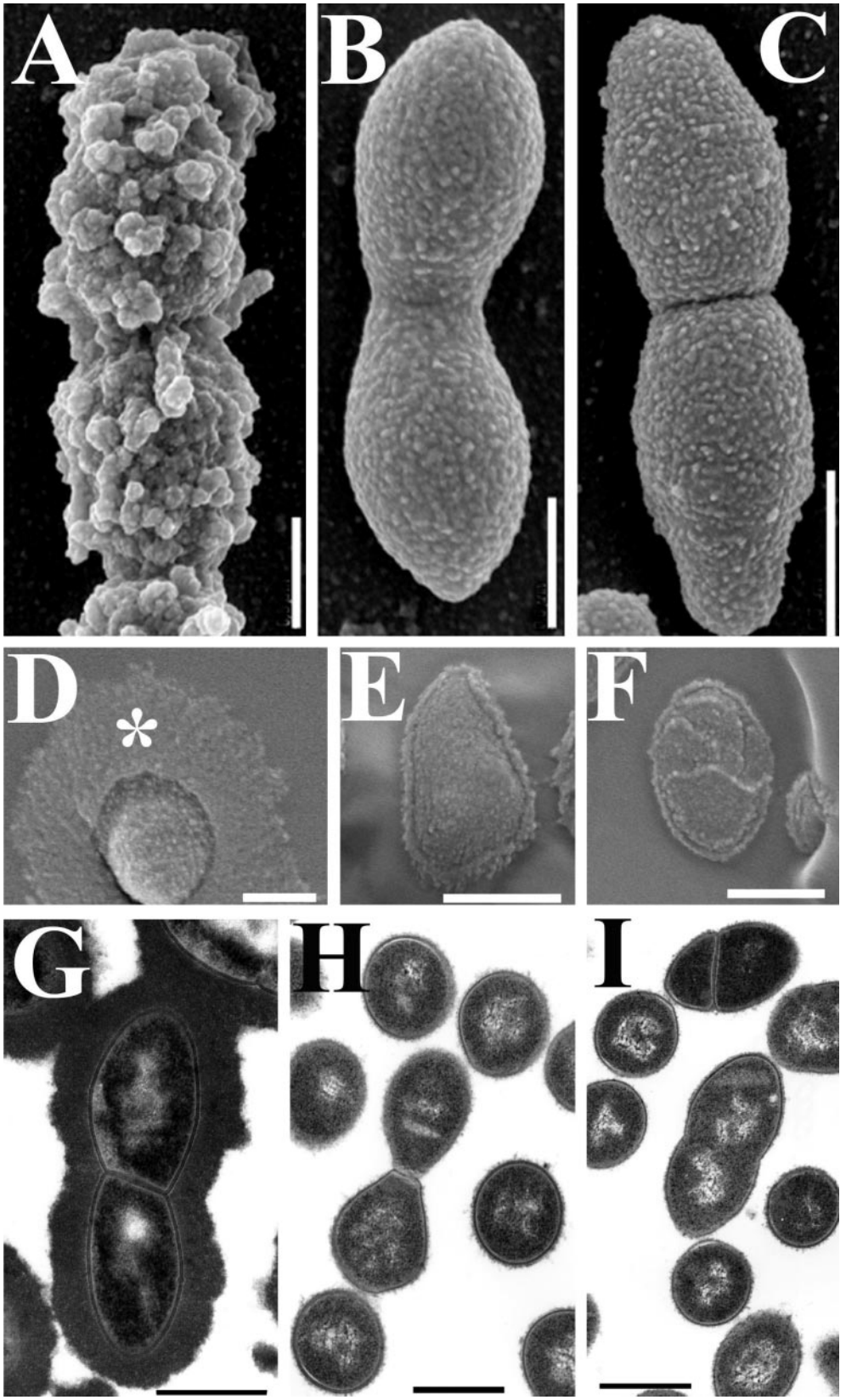

FIG. 3. Comparison of capsular structures of serotype 3 strain A66 and recovered pneumococci. Pneumococcal variants of strain A66 recovered from HEp-2 cells (B, E, and H) and A459 cells (C, F, and I) were devoid of any visible capsular material, whereas strain A66 exhibited a dense capsular layer (A, D, and G). These observations were made by using three different methods, conventional FESEM (A to C), cryo-FESEM (D to F), and analysis of ultrathin sections (G to I) after LRR fixation. Bars = 0.5 μm.

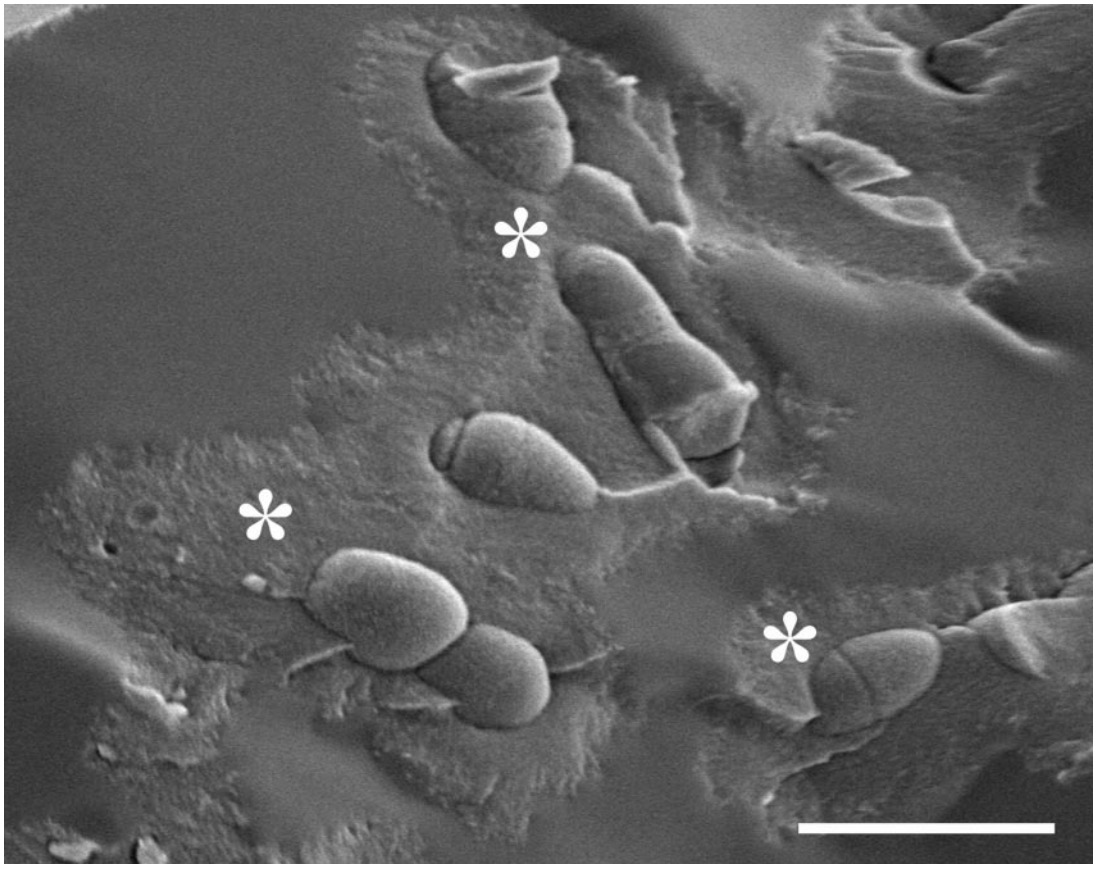

FIG. 4. Visualization of the vitrified pneumococcal capsule using cryo-FESEM after LRR fixation. Cryo-FESEM analysis revealed a dense thick capsule (asterisks) around serotype 3 strain A66, which is comparable to the capsule visualized in the ultrathin sections. Bar = 2 μm.

Fig. 7A, inset) and the capsule structure of pneumococci grown in DMEM (Fig. 7C). In contrast, after 1 h of adhesion we observed that for the pneumococci in intimate contact with the host cells the amount of capsular structure started to decrease (Fig. 7D and E) compared to the amount in other pneumococci in the attached chain or compared to DMEM-grown bacteria in which the capsule structure was rather similar along the entire chain (Fig. 7F). This observation was even more pronounced when longer infection times were studied. After 2 h of infection the attached pneumococci in close contact with the host cell membrane of the adherent chain exhibited an almost complete absence of capsular structure (Fig. 7G and H). The inset in Fig. 7G shows an ultrathin section of an adherent A66 cell embedded by using the LRR fixation protocol, which demonstrated the loss of the capsular material. All other pneumococci in this chain showed capsule structures (Fig. 7G), as did a pneumococcal chain grown for 2 h in DMEM (Fig. 7I). The amount of polysaccharide capsule was greatly reduced for all adherent pneumococci which were in contact with the host cell, as shown in Fig. 7L. Three hours after infection only the pneumococci in intimate contact with the host cell membrane were devoid of capsular structure, whereas the remaining pneumococci in the attached chain expressed a thick layer of capsule (Fig. 7J, K, and M). Pneumococci grown in DMEM again showed expression of capsular material over the entire chain (data not shown). Ultrathin section analysis again indicated that adherent bacteria lost the capsular structure, whereas bacteria not in close contact still retained the capsule (Fig. 7M, inset, and Fig. 8D and E).

When infected host cells were treated with 0.05% Triton X-100 for 5 min followed by LRR fixation, we were able to observe attached and invading pneumococcal chains. As deduced from Fig. 7N, adherent pneumococci in close contact with the host cell membrane and invading pneumococci did not exhibit a visible capsular structure, whereas pneumococci not in close contact with the host membrane exhibited the typical capsular structure after LRR fixation and preparation for FESEM. Pneumococci residing inside host cells (Fig. 7O) showed no detectable capsular polysaccharide material.

This suggests that pneumococci that express a reduced amount of capsular polysaccharide and are in close contact with the cells are not representatives of acapsular mutants that might have been enriched during growth and infection. Invasive bacteria recovered from epithelial cells by the gentamicin assay may nevertheless represent spontaneous mutants enriched during cultivation.

Pneumococcal encapsulation in mouse lung tissue. Mice were intranasally challenged with *S. pneumoniae* serotype 3 strain A66, and the lungs were processed for morphological analysis by the LRR fixation method and embedded in an acrylic resin (LRWhite). As shown in Fig. 8, pneumococci were localized in spatial distance from the cells (Fig. 8A) and in

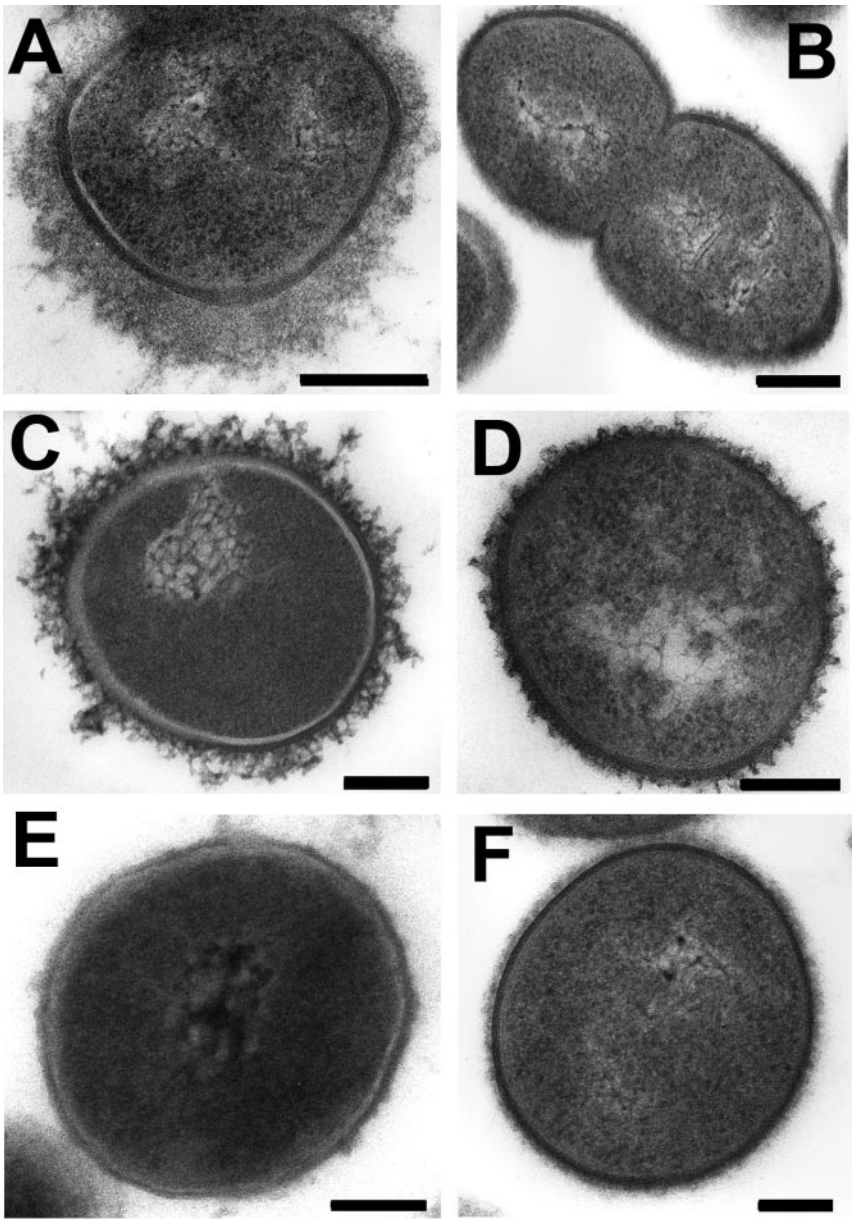

FIG. 5. Capsular structures in different serotypes. LRR fixation allowed detection of capsular structures in serotype 1 (wild-type strain P53) (A) and serotype 19F (wild-type strain P91) (C). Furthermore, the fixation protocol unequivocally demonstrated the absence of capsular material in the isolated intracellular variants of serotype 1 (B), loss of capsular material in variants of serotype 19F (D), and the absence of capsular structures in nonencapsulated strains R6x (E) and R800 (F). Bars = 0.25 μm.

contact with lung epithelial tissue (Fig. 8D and E). The LRR fixation successfully stabilized and preserved the polysaccharide capsule of pneumococci in lung tissue (Fig. 8A to D). FESEM indicated that pneumococci expressed the capsule in the environment of the lung tissue (Fig. 8A, B, and C), whereas bacteria which were in contact with lung epithelial tissue showed a drastic reduction in the density of the capsular polysaccharide layer (Fig. 8D and E). These in vivo results obtained with a mouse model provide further evidence for the observation that the amount of polysaccharide of pneumococci in intimate contact with host cells is reduced.

DISCUSSION

The capsular polysaccharide represents one of the most important pneumococcal virulence factors and is differentially regulated in different host habitats (35). Different phenotypes of a pathogen contribute to colonization, survival, or dissemination. Several studies have suggested that the capsule prevents attachment of pneumococci to epithelial cells, as well as to endothelial cells (1, 38, 42, 50, 52). The transparent phenotype, which produces smaller amounts of capsular polysaccharide, was shown to be more efficient in colonizing mucosal

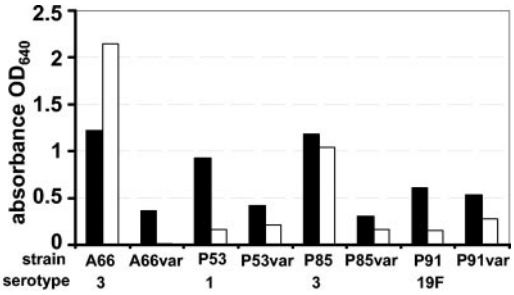

FIG. 6. Quantification of bacterium-associated polysaccharides or polysaccharides in culture supernatants. The differences in bacterium-associated polysaccharides (solid bars) or polysaccharides in the culture supernatants (open bars) were assessed for wild-type pneumococci and pneumococcal variants (var) recovered from epithelial cells. The total amount of acidic polysaccharides (bacterium associated or in the supernatant) was measured by determining the optical density at 640 nm (OD_{640}).

surfaces of the nasopharynx and in residing on surfaces, whereas the opaque phenotype is more virulent in systemic infections (26, 50–53). In epidemiological studies nontypeable, nonencapsulated nasopharyngeal carrier strains were identified, and one group of these organisms was genetically closely related to encapsulated strains (24, 54). In addition to elucidation of gene expression profiles during pathogenesis, it is necessary to visualize phenotypic changes of subcellular structures during infectious processes. The analysis of phenotypes should provide insights into the mechanism(s) facilitating adaptation of pathogens to their host niches. In this study the capsular polysaccharides of different pneumococcal serotypes were examined in vitro and in vivo by using a modified fixation method for electron microscopic studies which preserved the capsular material. Differences in the amount of capsular polysaccharide were shown to affect adherence and invasion substantially.

The capsular polysaccharide is highly hydrated and contains numerous anionic charged sites. Preservation and visualization of the capsular material in electron microscopic studies were achieved by using the cationic reagent ruthenium red in the fixation protocols. Ruthenium red has been used previously to visualize the capsule of *S. pneumoniae* and *Klebsiella pneumoniae* (40). Nevertheless, the fixation protocol mentioned above resulted in inadequate stabilization of the pneumococcal capsule. A lysine-based aldehyde-ruthenium red fixation protocol resulted in very stable preservation of the staphylococcal glycocalyx (15, 16). This LRR fixation protocol resulted in substantially improved preservation of the pneumococcal capsule and diminished the partially fuzzy and fibrous appearance of the capsule observed in the absence of lysine. As a result, the LRR fixation procedure allowed for the first time observation of the dynamic process of capsule expression on the bacterial surface of attaching and invading pneumococci by high-resolution FESEM, thereby discriminating between highly encapsulated and weakly encapsulated bacteria. There is no need for capsule-specific antibodies, and the method can be applied to all pneumococcal serotypes. Moreover, this fixation method can also be employed to preserve and stabilize polysaccharides of other pathogens, such as *Streptococcus pyogenes* (data not shown). When the LRR fixation method is used, the thickness of bacterium-associated carbohydrate structures can be monitored. This is especially of interest for phenotypic analysis of pathogens residing in different host niches, as demonstrated for pneumococci colonizing the lung epithelial tissue of mice.

When epithelial cells were infected with *S. pneumoniae* serotype 3 strain A66, bacteria recovered from the invasion experiments lacked the mucoid phenotype on blood agar, and, as demonstrated by electron microscopy, the thickness of the capsule was substantially reduced. These variants were substantially attenuated in a sepsis mouse model of infection and were able to revert in vivo to full encapsulation (data not shown). In a model of intranasal infection the wild type, as well as revertants, showed a higher colonization rate than the variants (data not shown). Both the in vitro and in vivo experiments revealed a reduced amount of capsular material of pneumococci attaching to the cells. The electron microscopic studies of pneumococci colonizing the murine lung tissue and the intranasal infections revealed a substantially reduced thickness for the capsular polysaccharide during invasion and a smaller amount of capsule during colonization. This study confirmed, therefore, the results of a previous study which showed that in a murine model of infection type 3 strains with only 20% of the capsular material colonize as effectively as the parental strain and remain highly virulent. Pneumococci that produced less than 6% of the capsular material were not able to colonize mice (30). Morphological analysis of the amount of capsule expressed performed by electron microscopy illustrated for the first time that the thickness of the capsule is reduced upon adherence of pneumococci to epithelial cells. The reduced amount of capsule promotes colonization, results in exposure of adhesive molecules, and allows the pathogen to strengthen the intimate contact with the epithelial cells and its subsequent uptake.

The reduced amount of capsule during intimate contact with the host cells is a double-edged sword for the pneumococcus. It is well established that differences in the amount of capsular polysaccharide have a major impact on virulence (3, 5, 31). A reduction in the amount of capsular material might strongly enhance adherence and uptake. But the reduced amount of capsule might convert the pneumococcus into a more apathogenic state in terms of its ability to evade the immune system. Therefore, the conversion from highly encapsulated to less encapsulated pneumococci and also the retrograde conversion must be sensitively regulated in order to enable the pathogen to colonize, survive, and disseminate within the human host.

Phenotypic alterations are usually random (13), but environmental conditions may also modulate these events (7, 19, 22). *S. pneumoniae* clinical isolates derived from different host environments have phenotypic differences. The mechanisms and environmental conditions which influence capsular polysaccharide expression are not well defined. In aerobic microenvironments like mucosal airway surfaces the inhibitory effect of oxygen suppresses production of capsular polysaccharide, supporting the finding that environmental pressure selects for distinct subpopulations of pneumococci (53). The inhibitory effect was correlated with decreased tyrosine phosphorylation of CpsD, which is an autophosphorylating protein-tyrosine kinase and regulator of capsular polysaccharide synthesis (30, 32, 53). In sorbarod biofilms, which were used to mimic the conditions of the different host microenvironments, such as naso-

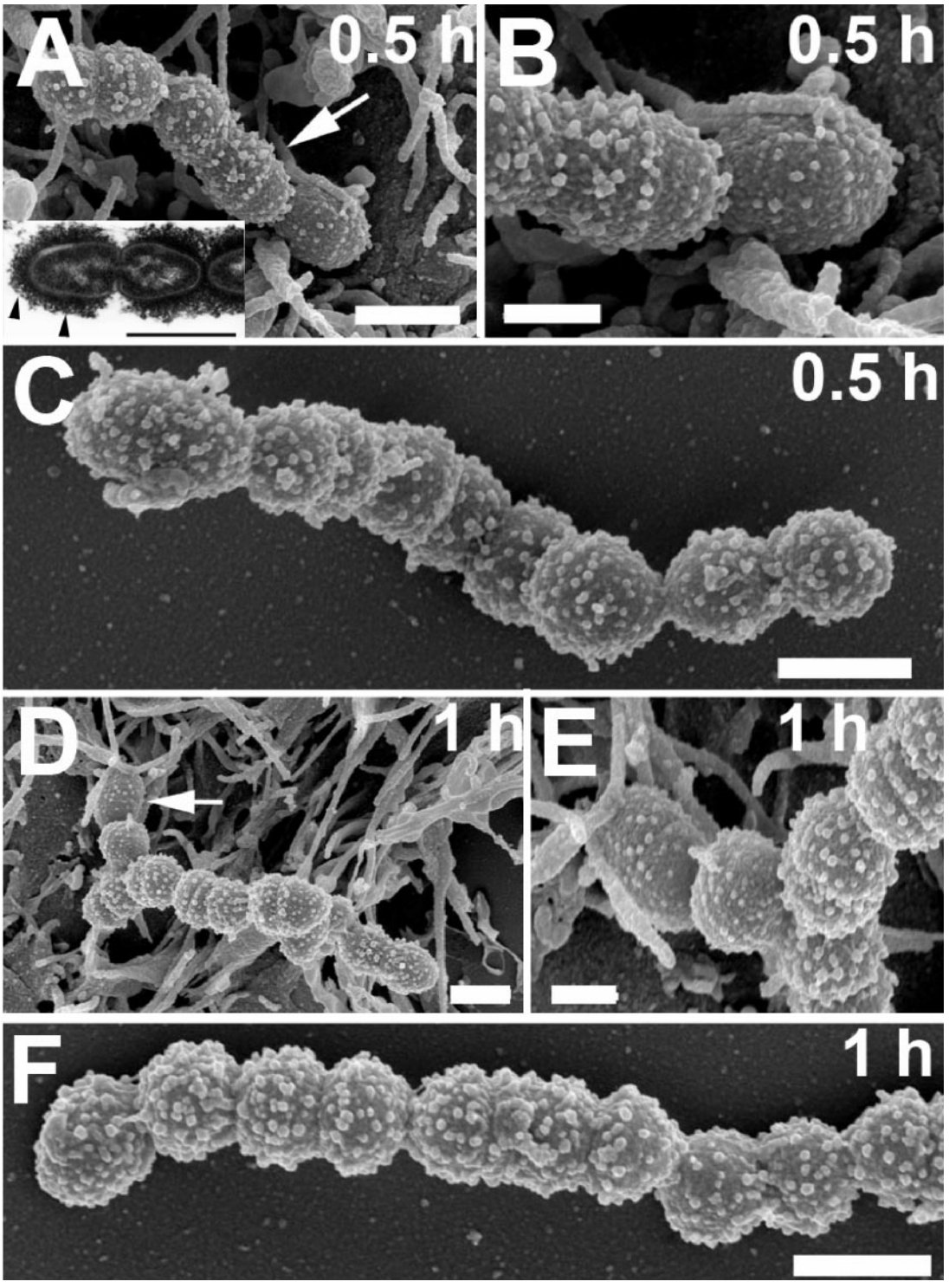

FIG. 7. Time series of capsule modulation during adhesion and invasion as visualized by FESEM. Monolayers of HEp-2 cells were infected with strain A66 and fixed by using the LRR protocol. The time series revealed that during adhesion to HEp-2 cells the pneumococcal capsule of serotype 3 strain A66 (= NCTC7978) was downregulated only on pneumococcal cells which were in intimate contact with the host cell membrane (arrows in panels A, D, G, J, L, and M; also higher magnifications of the region are shown in panels B, E, H, and K). The remaining bacteria in the attached chains (A, D, G, J, and M) or DMEM-grown pneumococci (C, F, and I) exhibit a dense layer of capsular material. Triton X-100-treated infected HEp-2 cells also demonstrated that pneumococci in close contact with the host cell membrane have highly downregulated capsules (N) and that invading pneumococci (N), as well as intracellular pneumococci (O), also have a substantially reduced capsule. The insets in panels A, G, and M show ultrathin sections of LRR-fixed samples, demonstrating the loss of capsular structure during the adherence and invasion process, whereas nonadherent bacteria exhibit a dense capsular structure (arrowheads in panels A and M). Bars = 1 μm.

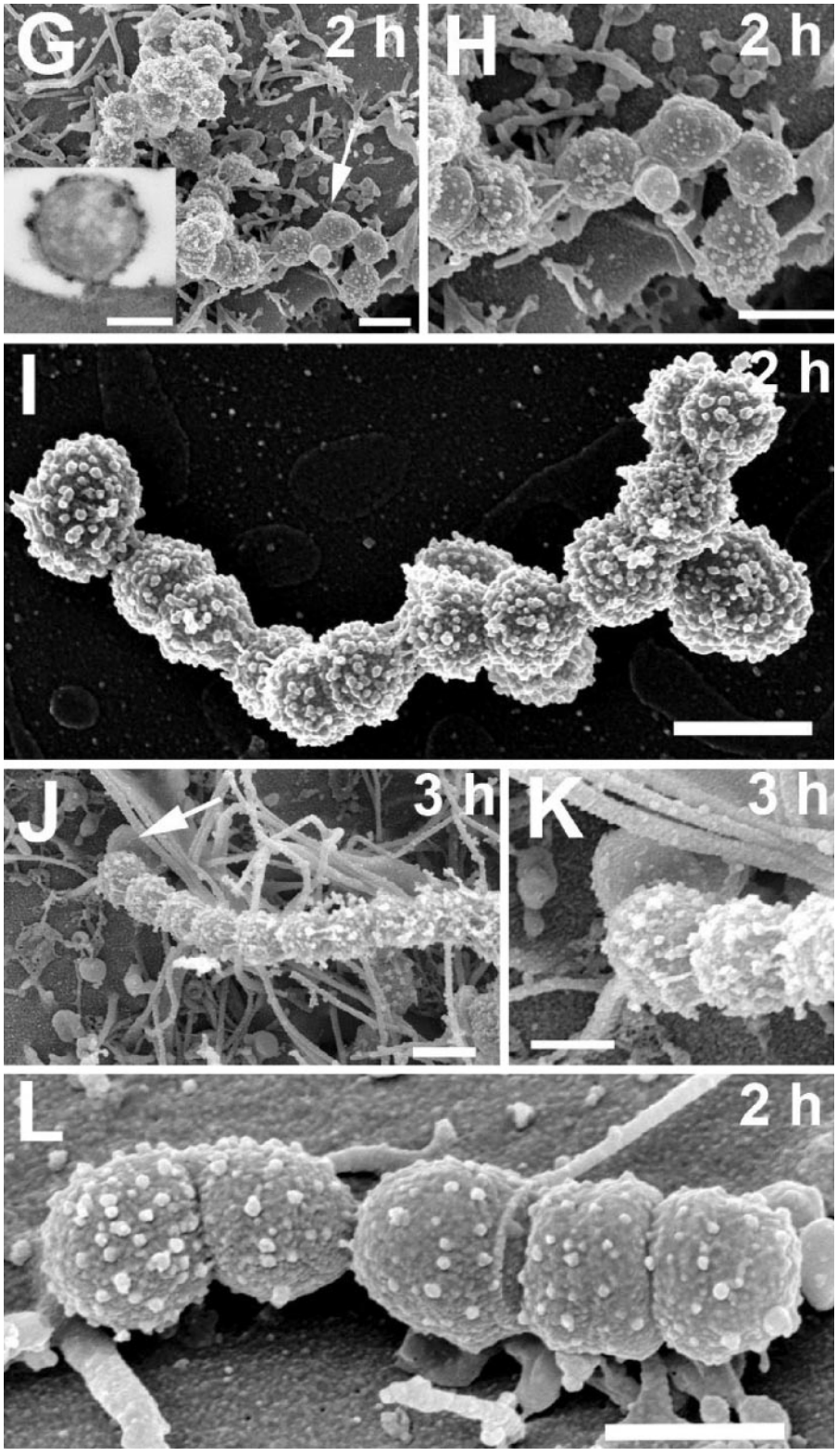

FIG. 7—*Continued.*

pharyngeal carriage, serotype 3 pneumococci generated spontaneous sequence duplications within the *cps3D* (*cap3A*) gene of the type 3 capsule locus, thereby causing high-frequency capsule phase variations (47). Recently, this effect was also described for pneumococci in sorbarod cultures of serotypes 8 and 37 (48). Cps3D, which is a UDP-glucose dehydrogenase and converts UDP-glucose to UDP-glucuronic acid, and Cps3S, which is a type 3 polysaccharide synthase, are required

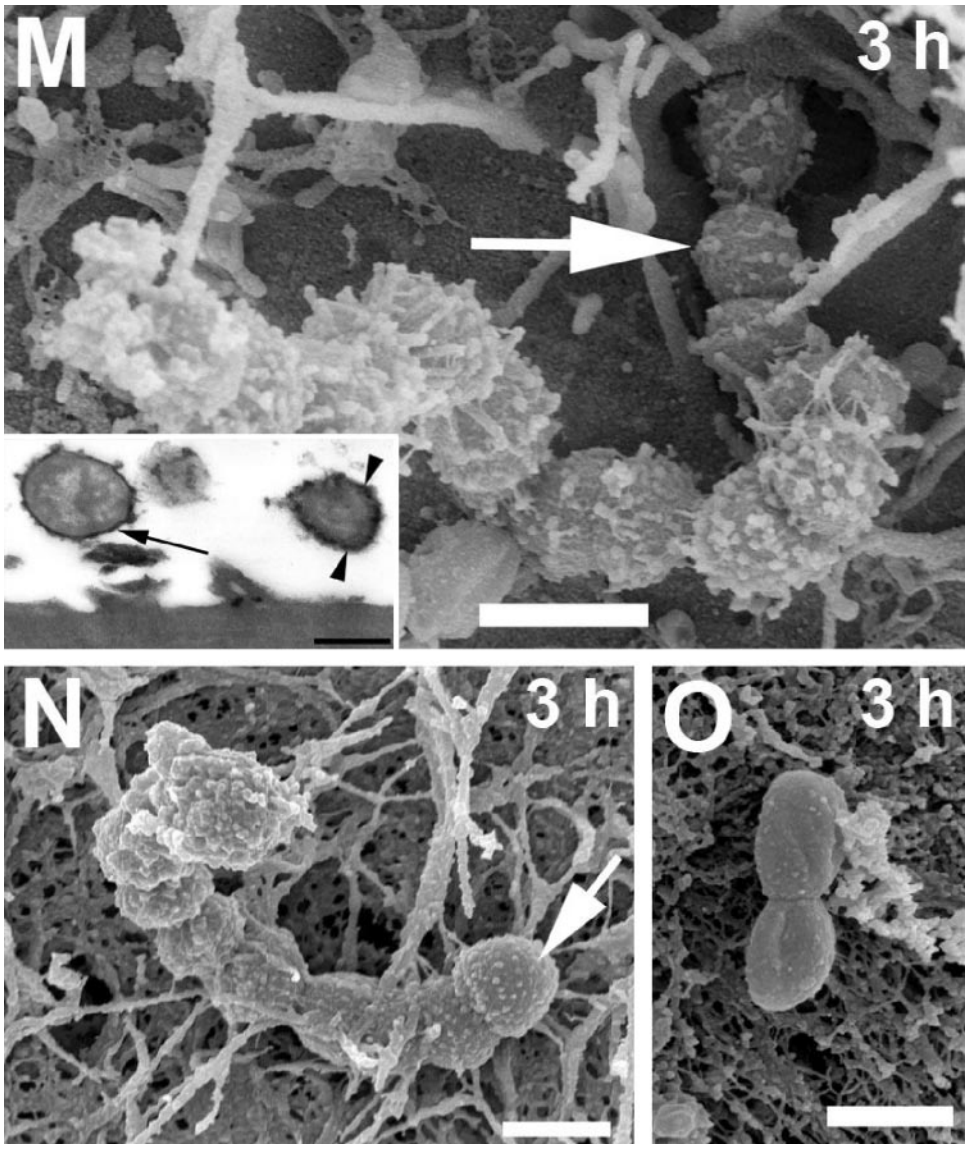

FIG. 7—*Continued.*

for synthesis of type 3 capsule (2, 12). Mutations in these type 3-specific genes of the type 3 capsule locus, which is transcribed as a single operon, *cps3DSUM-tnpA-plpA*, have been found to alter capsule production. Other studies showed that the frequency of spontaneous mutations in pneumococcal genes is influenced by endogenous hydrogen peroxide production (36, 37).

Our studies were unable to address precisely the underlying molecular mechanisms of the phenomenon observed. Northern blot experiments showed that the expression of serotype 3-specific genes in the variants is identical to that in the parental serotype 3 strain (data not shown). Furthermore, none of the other transcripts of pneumococcal virulence factors examined, such as PspA, SpsA (also referred to as CbpA and PspC), and PavA, was changed (data not shown). Sequence analysis of the type 3 capsule locus and the gene encoding phosphoglucomutase for 25 variants randomly isolated from three different in vitro experiments revealed that in 56% of the cases there were no changes in the sequence of the type-specific genes. The *pgm* sequence was not affected at all. Mutations in *pgm* have been shown to reduce capsule production in a type 3 strain (23). In the remaining variants a mutation of a single base pair generated a premature stop codon in *cps3D* and disrupted the function of Cps3D (data not shown).

It seems obvious that genes outside the type 3 capsule locus are essential for capsule biosynthesis and regulation. Standardized in vivo and in vitro models of infection are required to identify the predominant mechanisms of capsule regulation and environmental stimuli which alter capsule expression. These models should ideally reflect the situations and conditions during nasopharyngeal carriage and uptake into the host cells, with subsequent contact with the submucosa or even the blood. Exploitation of live imaging or electron microscopy for the analysis of phenotypic variations and molecular analysis should contribute to elucidation of the biologically significant

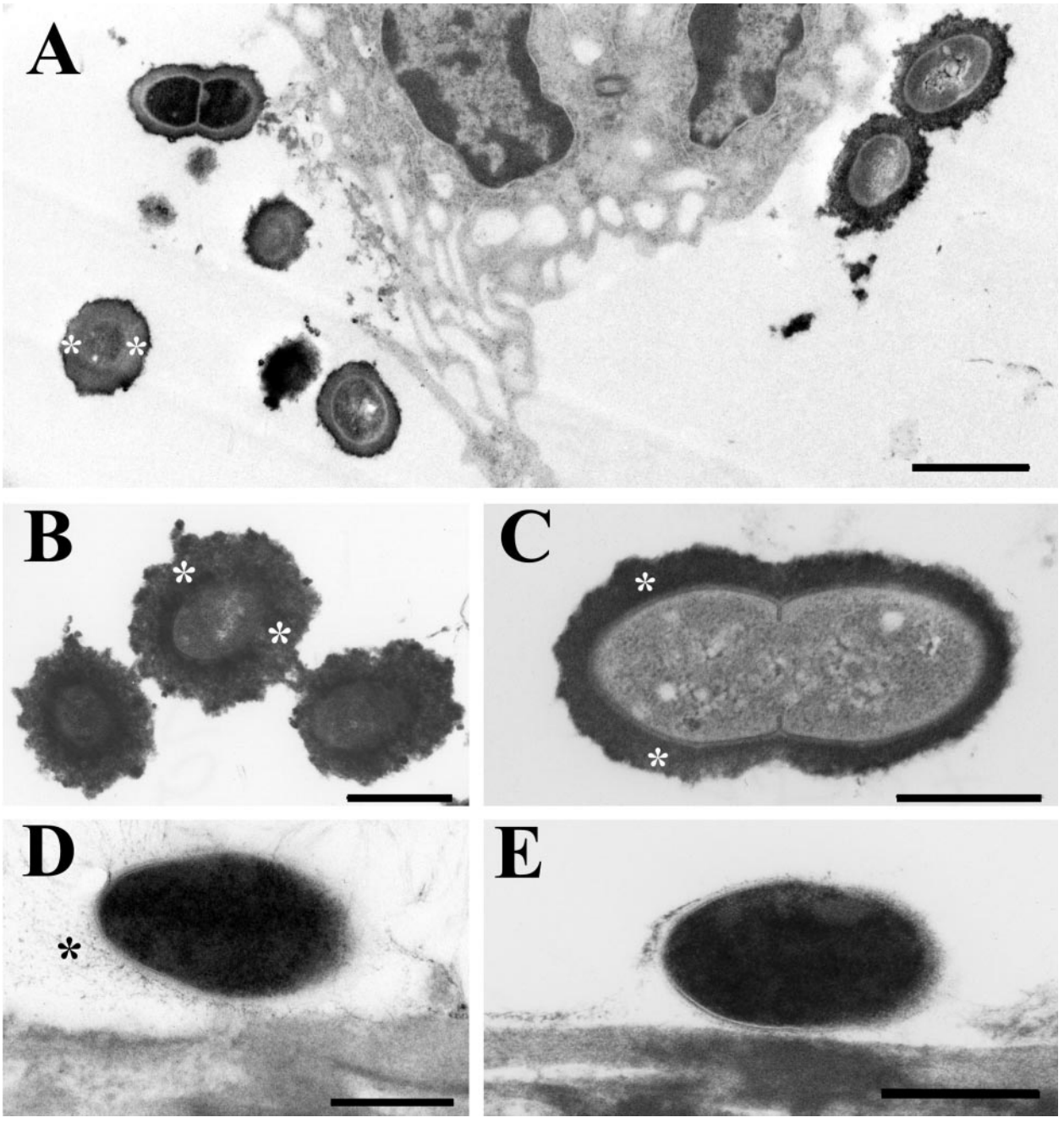

FIG. 8. Polysaccharide capsule in vivo in lung tissue of mice. C57BL/6 mice were intranasally challenged with 5×10^6 CFU of serotype 3 *S. pneumoniae* strain A66. Infected mice were sacrificed after 3 h, and lungs were LRR fixed. Capsular polysaccharide was preserved in the environment of the lung epithelium tissue (A, B, and C). The capsule is indicated by asterisks. Only pneumococci in intimate contact with lung cells showed a reduced density of capsular polysaccharide or were devoid of capsular material (D and E). (A) Bar = 1 μm. (B to E) Bars = 0.5 μm.

mechanisms. Moreover, isolation of carrier and invasive pneumococci of clonal origin from patients suffering from pneumococcal diseases and phenotypic as well as genetic analyses are required to correlate the in vitro data with the in vivo situation. The findings might also provide insight into the mechanisms which favor outbreaks of pneumococcal diseases.

ACKNOWLEDGMENTS

We acknowledge P. Matzander and D. McMillan (GBF) for critical reading of the manuscript, Astrid Müller (GBF), Ina Schleicher (GBF), and Christa Albert (Research Center for Infectious Diseases) for technical assistance, and R. R. Reinert (Medical University of Aachen) for serotyping.

This work was partially supported by the Deutsche Forschungsgemeinschaft (Sonderforschungsbereich 479 TP A7 to S.H.; grant Ro-2407/1 to M.R.) and by grants from the Federal Ministry for Education and Research to S.H. (grant BMBF-CAPNETZ C8) and S.R. (grant BMBF-CAPNETZ C4).

REFERENCES

1. **Adamou, J. E., T. M. Wizemann, P. Barren, and S. Langermann.** 1998. Adherence of *Streptococcus pneumoniae* to human bronchial epithelial cells (BEAS-2B). Infect. Immun. **66:**820–822.
2. **Arrecubieta, C., E. Garcia, and R. Lopez.** 1995. Sequence and transcriptional analysis of a DNA region involved in the production of capsular polysaccharide in *Streptococcus pneumoniae* type 3. Gene **167:**1–7.
3. **Austrian, R.** 1981. Some observations on the pneumococcus and the current status of pneumococcal disease and its prevention. Rev. Infect. Dis. **3:**S1–S17.
4. **Austrian, R.** 1986. Some aspects of the pneumococcal carrier state. J. Antimicrob. Chemother. **18**(Suppl. A)**:**35–45.
5. **Avery, O. T., and R. Dubos.** 1931. The protective action of a specific enzyme against type III pneumococcus in mice. J. Exp. Med. **54:**73–89.
6. **Avery, O. T., C. M. MacLeod, and M. McCarty.** 1944. Studies on the chemical nature of the substance inducing transformation by a desoxyribonucleic acid fraction isolated from pneumococcus type III. J. Exp. Med. **79:**137–158.
7. **Blyn, L. B., B. A. Braaten, and D. A. Low.** 1990. Regulation of pap pilin phase variation by a mechanism involving differential dam methylation states. EMBO J. **9:**4045–4054.
8. **Brown, E. J.** 1985. Interaction of gram-positive microorganisms with complement. Curr. Top. Microbiol. Immunol. **121:**159–187.
9. **Cartwright, K.** 2002. Pneumococcal disease in Western Europe: burden of disease, antibiotic resistance and management. Eur. J. Pediatr. **161:**188–195.
10. **Coffey, T. J., M. C. Enright, M. Daniels, J. K. Morona, R. Morona, W. Hryniewicz, J. C. Paton, and B. G. Spratt.** 1998. Recombinational exchanges at the capsular polysaccharide biosynthetic locus lead to frequent serotype changes among natural isolates of *Streptococcus pneumoniae*. Mol. Microbiol. **27:**73–83.
11. **Cundell, D. R., N. P. Gerard, C. Gerard, I. Idanpaan-Heikkila, and E. I. Tuomanen.** 1995. *Streptococcus pneumoniae* anchor to activated human cells by the receptor for platelet-activating factor. Nature **377:**435–438.
12. **Dillard, J. P., and J. Yother.** 1994. Genetic and molecular characterization of capsular polysaccharide biosynthesis in *Streptococcus pneumoniae* type 3. Mol. Microbiol. **12:**959–972.
13. **Dybvig, K.** 1993. DNA rearrangements and phenotypic switching in prokaryotes. Mol. Microbiol. **10:**465–471.
14. **Elm, C., R. Braathen, S. Bergmann, R. Frank, J. P. Vaerman, C. S. Kaetzel, G. S. Chhatwal, F. E. Johansen, and S. Hammerschmidt.** 2004. Ectodomains 3 and 4 of human polymeric immunoglobulin receptor (hpIgR) mediate invasion of *Streptococcus pneumoniae* into the epithelium. J. Biol. Chem. **279:**6296–6304.
15. **Fassel, T. A., P. E. Mozdziak, J. R. Sanger, and C. E. Edmiston, Jr.** 1997. Paraformaldehyde effect on ruthenium red and lysine preservation and staining of the staphylococcal glycocalyx. Microsc. Res. Tech. **36:**422–427.
16. **Fassel, T. A., P. E. Mozdziak, J. R. Sanger, and C. E. Edmiston, Jr.** 1998. Superior preservation of the staphylococcal glycocalyx with aldehyde-ruthenium red and select lysine salts using extended fixation times. Microsc. Res. Tech. **41:**291–297.
17. **Fassel, T. A., and C. E. Edmiston, Jr.** 1999. Ruthenium red and the bacterial glycocalyx. Rev. Biotechnol. Histochem **74:**194–212.
18. **Finlay, B. B., and S. Falkow.** 1989. Common themes in microbial pathogenicity. Microbiol. Rev. **53:**210–230.
19. **Gally, D. L., J. A. Bogan, B. I. Eisenstein, and I. C. Blomfield.** 1993. Environmental regulation of the *fim* switch controlling type 1 fimbrial phase variation in *Escherichia coli* K-12: effects of temperature and media. J. Bacteriol. **175:**6186–6193.
20. **Gillespie, S. H.** 1989. Aspects of pneumococcal infection including bacterial virulence, host response and vaccination. J. Med. Microbiol. **28:**237–248.
21. **Hammerschmidt, S., A. Muller, H. Sillmann, M. Muhlenhoff, R. Borrow, A. Fox, J. van Putten, W. D. Zollinger, R. Gerardy-Schahn, and M. Frosch.** 1996. Capsule phase variation in *Neisseria meningitidis* serogroup B by slipped-strand mispairing in the polysialyltransferase gene (*siaD*): correlation with bacterial invasion and the outbreak of meningococcal disease. Mol. Microbiol. **20:**1211–1220.
22. **Hardy, G. G., A. D. Magee, C. L. Ventura, M. J. Caimano, and J. Yother.** 2001. Essential role for cellular phosphoglucomutase in virulence of type 3 *Streptococcus pneumoniae*. Infect. Immun. **69:**2309–2317.
23. **Hardy, G. G., M. J. Caimano, and J. Yother.** 2000. Capsule biosynthesis and basic metabolism in *Streptococcus pneumoniae* are linked through the cellular phophoglucomutase. J. Bacteriol. **182:**1854–1863.
24. **Hathaway, L. J., P. Stutzmann Meier, P. Battig, S. Aebi, and K. Muhlemann.** 2004. A homologue of *aliB* is found in the capsule region of noncapsulated *Streptococcus pneumoniae*. J. Bacteriol. **186:**3721–3729.
25. **Kelly, T., J. P. Dillard, and J. Yother.** 1994. Effect of genetic switching of capsular type on virulence of *Streptococcus pneumoniae*. Infect. Immun. **62:**1813–1819.
26. **Kim, J. O., and J. N. Weiser.** 1998. Association of intrastrain phase variation in quantity of capsular polysaccharide and teichoic acid with the virulence of *Streptococcus pneumoniae*. J. Infect. Dis. **177:**368–377.
27. **Lacks, S. A., and R. D. Hotchkiss.** 1960. A study of the genetic material determining an enzyme activity in pneumococcus. Biochim. Biophys. Acta **39:**508–517.
28. **Luft, J. H.** 1971. Ruthenium red and violet. 1. Chemistry, purification, methods of use for electron microscopy and mechanism of action. Anat. Rec. **171:**347–368.
29. **Luft, J. H.** 1971. Ruthenium red and violet. II. Fine structural localization in animal tissue. Anat. Rec. **171:**369–415.
30. **Magee, A. D., and J. Yother.** 2001. Requirement for capsule in colonization by *Streptococcus pneumoniae*. Infect. Immun. **69:**3755–3761.
31. **McLeod, C. M., and M. R. Krauss.** 1950. Relation of virulence of pneumococcal strains for mice to the quantity of capsular polysaccharide formed in vitro. J. Exp. Med. **92:**1–9.
32. **Morona, J. K., J. C. Paton, D. C. Miller, and R. Morona.** 2000. Tyrosine phosphorylation of CpsD negatively regulates capsular polysaccharide biosynthesis in *Streptococcus pneumoniae*. Mol. Microbiol. **35:**1431–1442.
33. **Mulholland, K.** 1999. Strategies for the control of pneumococcal diseases. Vaccine **17**(Suppl. 1)**:**S79–S84.
34. **Musher, D. M.** 1992. Infections caused by *Streptococcus pneumoniae*: clinical spectrum, pathogenesis, immunity, and treatment. Clin. Infect. Dis. **14:**801–807.
35. **Ogunniyi, A. D., P. Giammarinaro, and J. C. Paton.** 2002. The genes encoding virulence-associated proteins and the capsule of *Streptococcus pneumoniae* are upregulated and differentially expressed in vivo. Microbiology **148:**2045–2053.
36. **Pericone, C. D., K. Overweg, P. W. Hermans, and J. N. Weiser.** 2000. Inhibitory and bactericidal effects of hydrogen peroxide production by *Streptococcus pneumoniae* on other inhabitants of the upper respiratory tract. Infect. Immun. **68:**3990–3997.
37. **Pericone, C. D., D. Bae, M. Shchepetov, T. McCool, and J. N. Weiser.** 2002. Short-sequence tandem and nontandem DNA repeats and endogenous hydrogen peroxide production contribute to genetic instability of *Streptococcus pneumoniae*. J. Bacteriol. **184:**4392–4399.
38. **Ring, A., J. N. Weiser, and E. I. Tuomanen.** 1998. Pneumococcal trafficking across the blood-brain barrier. Molecular analysis of a novel bidirectional pathway. J. Clin. Investig. **102:**347–360.
39. **Schrager, H. M., J. G. Rheinwald, and M. R. Wessels.** 1996. Hyaluronic acid capsule and the role of streptococcal entry into keratinocytes in invasive skin infection. J. Clin. Investig. **98:**1954–1958.
40. **Springer, E. L., and I. L. Roth.** 1973. The ultrastructure of the capsules of *Diplococcus pneumoniae* and *Klebsiella pneumoniae* stained with ruthenium red. J. Gen. Microbiol. **74:**21–31.
41. **Spurr, A. R.** 1969. A low-viscosity epoxy resin embedding medium for electron microscopy. J. Ultrastruct. Res. **26:**31–43.
42. **Talbot, U. M., A. W. Paton, and J. C. Paton.** 1996. Uptake of *Streptococcus pneumoniae* by respiratory epithelial cells. Infect. Immun. **64:**3772–3777.
43. **Tiraby, J. G., and M. S. Fox.** 1974. Marker discrimination and mutagen-induced alterations in pneumococcal transformation. Genetics **77:**449–458.
44. **Tong, H. H., J. N. Weiser, M. A. James, and T. F. DeMaria.** 2001. Effect of influenza A virus infection on nasopharyngeal colonization and otitis media induced by transparent or opaque phenotype variants of *Streptococcus pneumoniae* in the chinchilla model. Infect. Immun. **69:**602–606.
45. **Tuomanen, E. I., R. Austrian, and H. R. Masure.** 1995. Pathogenesis of pneumococcal infection. N. Engl. J. Med. **332:**1280–1284.
46. **van Dam, J. E., A. Fleer, and H. Snippe.** 1990. Immunogenicity and immunochemistry of *Streptococcus pneumoniae* capsular polysaccharides. Antonie Leeuwenhoek **58:**1–47.
47. **Waite, R. D., J. K. Struthers, and C. G. Dowson.** 2001. Spontaneous sequence duplication within an open reading frame of the pneumococcal type 3 capsule locus causes high-frequency phase variation. Mol. Microbiol. **42:**1223–1232.
48. **Waite, R. D., D. W. Penfold, J. K. Struthers, and C. G. Dowson.** 2003. Spontaneous sequence duplications within capsule genes *cap8E* and *tts* control phase variation in *Streptococcus pneumoniae* serotypes 8 and 37. Microbiology **149:**497–504.
49. **Watson, D. A., and D. M. Musher.** 1990. Interruption of capsule production in *Streptococcus pneumoniae* serotype 3 by insertion of transposon Tn*916*. Infect. Immun. **58:**3135–3138.
50. **Weiser, J. N., R. Austrian, P. K. Sreenivasan, and H. R. Masure.** 1994. Phase variation in pneumococcal opacity: relationship between colonial morphology and nasopharyngeal colonization. Infect. Immun. **62:**2582–2589.
51. **Weiser, J. N., Z. Markiewicz, E. I. Tuomanen, and J. H. Wani.** 1996. Relationship between phase variation in colony morphology, intrastrain variation in cell wall physiology, and nasopharyngeal colonization by *Streptococcus pneumoniae*. Infect. Immun. **64:**2240–2245.
52. **Weiser, J. N.** 2000. Phase variation of *Streptococcus pneumoniae*, p. 225–231.

In V. Fischetti, R. P. Novick, J. J. Ferretti, D. A. Portnoy, and J. I. Rood (ed.), Gram-positive pathogens. ASM Press, Washington, D.C.

53. **Weiser, J. N., D. Bae, H. Epino, S. B. Gordon, M. Kapoor, L. A. Zenewicz, and M. Shchepetov.** 2001. Changes in availability of oxygen accentuate differences in capsular polysaccharide expression by phenotypic variants and clinical isolates of *Streptococcus pneumoniae*. Infect. Immun. **69:**5430–5439.
54. **Whatmore, A. M., A. Efstratiou, A. P. Pickerill, K. Broughton, G. Woodard, D. Sturgeon, R. George, and C. G. Dowson.** 2000. Genetic relationships between clinical isolates of *Streptococcus pneumoniae*, *Streptococcus oralis*, and *Streptococcus mitis*: characterization of "atypical" pneumococci and organisms allied to *S. mitis* harboring *S. pneumoniae* virulence factor-encoding genes. Infect. Immun. **68:**1374–1382.
55. **Winkelstein, J. A.** 1984. Complement and the host's defense against the pneumococcus. Crit. Rev. Microbiol. **11:**187–208.
56. **Zhang, J. R., K. E. Mostov, M. E. Lamm, M. Nanno, S. Shimida, M. Ohwaki, and E. Tuomanen.** 2000. The polymeric immunoglobulin receptor translocates pneumococci across human nasopharyngeal epithelial cells. Cell **102:** 827–837.

Editor: J. N. Weiser